The AEgIS experiment

G. Testera[14] · S. Aghion[1,2] · C. Amsler[3] · A. Ariga[3] · T. Ariga[3] · A. Belov[4] · G. Bonomi[5,6] · P. Braunig[7] · J. Bremer[8] · R. Brusa[9,10] · L. Cabaret[11] · M. Caccia[2,12] · R. Caravita[13,14] · F. Castelli[2,15] · G. Cerchiari[16] · K. Chlouba[17] · S. Cialdi[2,15] · D. Comparat[11] · G. Consolati[1,2] · S. Curreli[14] · A. Demetrio[7] · H. Derking[8] · L. Di Noto[13,14] · M. Doser[8] · A. Dudarev[8] · A. Ereditato[3] · R. Ferragut[1,2] · A. Fontana[6] · S. Gerber[8] · M. Giammarchi[2] · A. Gligorova[18] · S. Gninenko[4] · S. Haider[8] · S. Hogan[19] · H. Holmestad[20] · T. Huse[20] · E. J. Jordan[16] · J. Kawada[3] · A. Kellerbauer[16] · M. Kimura[3] · D. Krasnický[13] · V. Lagomarsino[13,14] · S. Lehner[21] · C. Malbrunot[8,21] · S. Mariazzi[21] · V. Matveev[4] · Z. Mazzotta[15] · G. Nebbia[22] · P. Nedelec[23] · M. Oberthaler[7] · N. Pacifico[18] · L. Penasa[9,10] · V. Petracek[17] · C. Pistillo[3] · F. Prelz[2] · M. Prevedelli[24] · L. Ravelli[9,10] · C. Riccardi[6,25] · O. M. Røhne[20] · S. Rosenberger[8] · A. Rotondi[6,25] · H. Sandaker[18] · R. Santoro[2,12] · P. Scampoli[3] · L. Semeria[14] · M. Simon[21] · M. Spacek[17] · J. Storey[3] · I. M. Strojek[17] · M. Subieta[5,6] · E. Widmann[21] · P. Yzombard[11] · S. Zavatarelli[14] · J. Zmeskal[21] · (AEgIS Collaboration)

Published online: 27 March 2015

✉ G. Testera
testera@ge.infn.it

1 Politecnico of Milano, Piazza Leonardo da Vinci 32, 20133 Milano, Italy

2 INFN Milano, via Celoria 16, 20133 Milano, Italy

3 Laboratory for High Energy Physics, Albert Einstein Center for Fundamental Physics, University of Bern, 3012 Bern, Switzerland

4 Institute for Nuclear Research of the Russian Academy of Science, Moscow 117312, Russia

5 Department of Mechanical and Industrial Engineering, University of Brescia, via Branze 38, 25123 Brescia, Italy

1 Introduction

General Relativity is based on the Equivalence Principle. The validity of this principle has been established over the years with extremely high accuracy and even more refined results are expected in the future. Particularly the universality of the free fall (UFF) has been verified with 10^{-13} accuracy [1]. However all these measurements are performed on matter systems and the validity of the equivalence principle for antimatter has never been directly tested. While a number of indirect and model dependent arguments disfavor a large violation for antimatter, models of quantum gravity [2] leave room for deviations. The availability of

[6] INFN Pavia, via Bassi 6, 27100 Pavia, Italy

[7] Kirchhoff-Institute for Physics, Heidelberg University, Im Neuenheimer Feld 227, 69120 Heidelberg, Germany

[8] Physics Department, CERN, 1211 Geneva 23, Switzerland

[9] Department of Physics, University of Trento, via Sommarive 14, 38123 Trento, Italy

[10] TIFPA/INFN Trento, via Sommarive 14, 38123 Trento, Italy

[11] Laboratory Aimé Cotton, CNRS, University of Paris-Sud, ENS Cachan, Bât. 505, 91405 Orsay, France

[12] Department of Science, University of Insubria, Via Valleggio 11, 22100 Como, Italy

[13] Department of Physics, University of Genova, via Dodecaneso 33, 16146 Genova, Italy

[14] Istituto Nazionale Fisica Nucleare, Via Dodecaneso 33, 16146 Genova, Italy

[15] Department of Physics, University of Milano, via Celoria 16, 20133 Milano, Italy

[16] Max Planck Institute for Nuclear Physics, Saupfercheckweg 1, 69117 Heidelberg, Germany

[17] Czech Technical University, Prague, Brehová 7, 11519 Prague 1, Czech Republic

[18] Institute of Physics and Technology, University of Bergen, Allégaten 55, 5007 Bergen, Norway

[19] University College London, Gower Street, London WC1E 6BT, UK

[20] Department of Physics, University of Oslo, Sem Sælandsvei 24, 0371 Oslo, Norway

[21] Stefan Meyer Institute for Subatomic Physics, Austrian Academy of Sciences, Boltzmanngasse 3, 1090 Vienna, Austria

[22] INFN Padova, via Marzolo 8, 35131 Padova, Italy

[23] Institute of Nuclear Physics, CNRS/IN2p3, University of Lyon 1, 69622 Villeurbanne, France

[24] University of Bologna, Viale Berti Pichat 6/2, 40126 Bologna, Italy

[25] Department of Physics, University of Pavia, via Bassi 6, 27100 Pavia, Italy

extremely cold antihydrogen atoms and the application of experimental techniques, which are well established for ultra-cold atoms, for antimatter atoms offer the possibility to perform high precision tests of the UFF for antimatter [3]. These measurements represent the long term goal of the AEgIS experiment. In its present first phase the AEgIS experiment is designed to measure the Earth's gravitational acceleration g of antihydrogen with an accuracy of about 1 % by detecting the vertical displacement of a cold ($\simeq$100 mK) beam flying through a moiré deflectometer. Even if reaching 1 % accuracy may appear a modest result compared with the accuracy reached for matter, this goal requires a formidable experimental effort to combine in a single apparatus several technologies developed in the field of the non neutral plasma manipulation, atomic physics, particle detectors. Note that, in some case, it is needed to go beyond the state of the art. A second goal of the experiment is to carry out spectroscopic measurements on the antihydrogen atoms in flight (particularly a measurement of the hyperfine splitting of antihydrogen).

The main part of the AEgIS apparatus is installed at CERN and is currently taking data. In this paper we summarise its main features and we report some selected results achieved during its commissioning.

2 The AEgIS apparatus and some selected results

Antihydrogen will be formed in AEgIS through the reaction of charge exchange between cold antiprotons and Rydberg positronium. Antiprotons delivered from AD (Antiproton Decelerator at CERN) are trapped and cooled in Penning-Malmberg traps. Rydberg positronium is formed by sending a short pulse (about 10 ns long) of about 10^8 positrons toward a nanoporous target [4, 5] and exciting the emerging positronium to selected Rydberg states by two laser pulses. Antihydrogen is formed in Rydberg states when positronium traverse the antiproton cloud. The main features of this production scheme are the pulsed production (the antihydrogen is formed within about 100 ns) and the fact that the antihydrogen temperature is determined by that of the antiprotons (expected to be 100 mK) before the charge exchange reaction. Note that in the usual antihydrogen production by recombination of antiprotons and positrons in nested traps, the antihydrogen is continuously produced during the time spent by the antiprotons in the nested trap (hundreds of ms or seconds) and that the temperature of the resulting antihydrogen depends on the competition between the antiproton cooling and recombination rates. A beam of antihydrogen with an horizontal velocity of few hundreds m/sec will be formed in AEgIS by fast applying to the trap electrodes suitable voltages creating a inhomogeneous electric field: the Rydberg anti-atoms will thus be accelerated in the horizontal direction [6]. The value of g will be obtained by the measuring the time of flight and the vertical displacement of the antiatoms after their flight through a moiré deflectometer working in the classical regime. The sensitivity of the measurement depends on the number of detected atoms and on the spatial resolution of the position sensitive detector [7]. The antihydrogen temperature must be as low as possible to limit the radial divergence of the beam. Efforts to get antiprotons with sub-Kelvin temperature are in progress [8, 9].

The experimental apparatus (shown in Fig. 1) is formed by a positron source and accumulator, a superconducting magnet allocating the Penning-Malmberg traps (main traps), a magnetic transfer line for transferring positrons from the accumulator to the main traps, several detectors mounted inside and outside the vacuum chambers, laser systems, the grating for the g measurement. The apparatus is installed and running at CERN with the exception of the grating system which is currently under design. In addition the apparatus includes

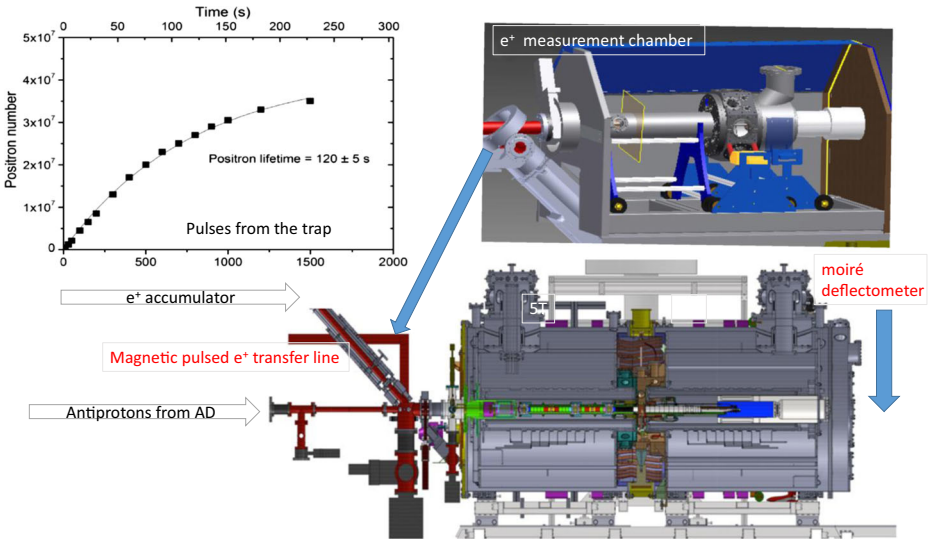

Fig. 1 The AEgIS apparatus. The positron measurement chamber is not to scale. The plot shows the number of accumulated positrons with a ^{22}Na source of 13.7 mCi

an external chamber allowing to perform measurements on positrons and positronium in absence of magnetic field without trapping them in the main traps. Data taking and commissioning with antiprotons started in 2012 and was continued during the year 2014 while during the year 2013 (when antiprotons were not available from AD) measurements with electrons and positrons were performed.

Positron accumulator The positron accumulator consists of a Surko type device [10] in which positrons emitted by a ^{22}Na radioactive source are moderate by a solid neon target and then trapped in a the first section of the device where a suitable pressure of the background gas allows their deceleration. Pulses of positrons are then extracted every few hundreds ms and trapped in the section of the apparatus called accumulator. The setup combines elements procured from the First Point Scientific company with and a high-quality ($\Delta B/B = 10^{-4}$) solenoidal magnet used in the accumulator and developed by us. The background pressure and the manipulation procedures in the accumulator are progressively optimised. Figure 1 shows the number of accumulated positrons as a function of the number of pulses from the first trap obtained with a 13.7 mCi source. Further improvements in alignment, shielding and process control, together with a stronger source, will allow to accumulate $2 \cdot 10^8$ positrons in few hundreds seconds. From the accumulator, positrons are extracted into the transfer line with 300 eV energy in pulses with of about 10 ns in duration. The transfer line maintains the 0.1 T magnetic field of the accumulator magnet throughout, and also allows horizontal extraction of positrons from the accumulator onto the separate positron experimental platform situated between the accumulator and the 5 T magnet.

The main traps The traps in the main magnet consist of a series of 105 cylindrical electrodes of varying length; part of them are located in the cold bore of the a 5 T magnetic field (trapping region) and the rest in the bore of the 1 Tesla (antihydrogen formation region) field. All the electrodes are individually biased to shape Penning or Malmberg traps of

variable length for trapping and manipulation of antiprotons, electrons and positrons (and also protons since a proton source is being installed). Some electrodes are radially split in 4 sectors permitting the application of radio-frequency voltages necessary to compress the trapped plasma (Rotating Wall). Antiprotons from AD are routinely trapped and cooled by collisions with electrons (confined together with antiprotons) in the trapping region: typically $1.2 \cdot 10^5$ antiprotons for each AD pulse are caught thanks to the 5 T field and the high voltage (9 kV) applied to the trap electrodes. Results are reported in [11].

The design of the electrodes located in the 1 Tesla field is not standard: in particular there is a "large radius trap" (2.2 cm radius while the electrodes of trapping region have 1.5 cm radius) connected with two series of electrodes (0.5 cm radius) mounted along two horizon-tal parallel axis. We call them on-axis trap and off-axis trap. The on-axis trap is mounted along the axis of the magnetic field and it is used to collect the antiprotons and cool them in the final region mounted below the nanoporous target. The electrodes facing the nanoporous target are realised with a grid on the top to allow the passage of the positronium. The grid is designed to optimise its transparency and minimise at the same time the distortion of the electric field due to the lack of rotational symmetry. Positrons and antiprotons are detected by several scintillators located around the apparatus. A double stage MCP (micro channel plate) coupled to a phosphor screen and a CCD camera is mounted in the fringe field of the 5 Tesla magnet along the path from AD to the main traps. This MCP is operated in a quite high magnetic field (about 2 Tesla) in a cryogenic environment and it is mounted on a mov-able support. A second MCP with phosphor screen is mounted in front of the last electrode of the on-axis trap. A Faraday cup not sectorized is mounted in front of the first electrode of the main trap also on a movable support. A radially sectorized Faraday cup is located in the middle of the two magnets with sectors collecting the plasma dumped from the 1 Tesla trap or from the 5 Tesla. Another movable support allows to place in position this Faraday cup or an electrode used during the transfer of the particles. Procedures for trapping, manip-ulation with rotating wall and transfer of particles among the various regions of the traps have been setup with electrons and are continuously improved. Figure 2 shows an example of results. In particular positrons arriving from the catching region must be first collected in the large radius trap and then they have to be moved across the magnetic field in the off-axis trap and launched toward the target. As reported in [12] the radial displacement of the plasma without altering its dimension can be obtained by excitation a particular plasma mode called diocotron mode. It consists in a radial displacement of the entire plasma col-umn and a rotation around the trap centre with the original plasma shape unchanged. The amplitude of the diocotron mode D is the distance of the plasma centre to the trap centre. We have used electrons (easily available in controlled number) to emulate the manipulation and off-axis displacement of positrons in the AEgIS apparatus. Typically $10^7 - 10^8$ elec-trons are trapped in the catching region in 5 T magnet and compressed. They are transferred into the large radius trap by adiabatically changing the voltages of the confining electrodes as necessary for positrons. In the large radius trap they are again compressed and then the diocotron mode is excited by applying radio-frequency voltages to a radial sector of one trap electrode. The frequency and amplitude of the signal are properly swept to match the expected diocotron frequency. To launch the particles toward the target we need to control D and the phase of the rotation. Figure 3 shows the results obtained in AEgIS by using the procedure described in detail in [12].

Antihydrogen detector A fast antihydrogen cryogenic (4 K) tracking detector is mounted around the antihydrogen formation region. It is designed to measure the time difference between the moment of formation and the moment of annihilation of antihydrogen on the

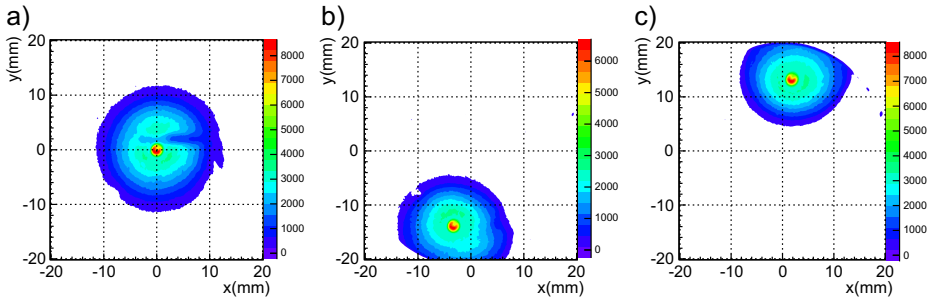

Fig. 2 Example of compression with rotating wall of a plasma of 2.6 10^8 electrons stored in the catching region. **a** no compression; **b** compression with a frequency of 1 MHz for 8 s; **c** typical result obtained after applying the rotating wall signal with 1 MHz for a time longer then 60 s. The final radius is about 0.5 mm

trap electrodes, as well as the position of the annihilation vertex along the horizontal z axis. The detector (20 cm long) consists of two double layers of Kuraray SCSF-78M multi-clad scintillating fibers (1 mm diameter). The 800 scintillating fibers are coupled to clear fibers that carry the signal to Hamamatsu Multi Pixel Photon Counters (MPPC) followed by an amplification stage. The MPPC are mounted in vacuum, while the amplifiers, together with the digital electronics that store the firing pattern of the scintillators with a frequency of 200 MHz for up to 10 s, are sited on the outside of the vacuum vessel. Based on Geant 4 simulations, a vertex resolution of 2.1 mm (along z) is expected. Tests with antiprotons began during the AEgIS run in 2012 and continued during the run in the year 2014.

Laser system The photo-excitation of positronium (Ps) to Rydberg states requires photon energies close to the binding energy of 6.8 eV. Laser systems at the corresponding wavelengths (180 nm) are not commercially available. We are therefore planning to perform a two-step excitation, from the ground state to the $n = 3$ state, and then to the $n = 26$ Rydberg band [13]. Two pulsed-laser systems, both of which are pumped by the same Nd:YAG laser, are mounted close to the main magnet. The pump laser of the whole system is a 650 mJ Q-switched Nd:YAG laser delivering a 4 ns pulse. The wavelengths are produced through second-order polarisation in optical crystals. The 205 nm radiation for the first transition is obtained by summing in a non-linear BBO crystal the 266 nm fourth harmonic of the 1064 nm Nd:YAG pulse and the 894 nm radiation (amplified by an optical parameter amplifier-OPA) generated in an optical parametric generator (OPG) by down-conversion of the second harmonic of the same laser. The other wavelength (around 1670 nm) is generated in a single step by an OPG starting from the same pump laser and then amplified by a second OPA system. Table 1 summarises some achieved results. A second laser system was developed for being used for experiments in the positron measurement chamber. Like the first one, this laser system will also reach the Rydberg states of Ps by two photon absorptions, but using the intermediate state n=2. In addition it can enable Doppler-free spectroscopy.

3 Toward the realisation of the grating and the position sensitive detector for the g measurement

Several ancillary measurements have been performed during the 2012 antiproton run testing various detectors with antiprotons with about 100 keV energy. In particular annihilations at

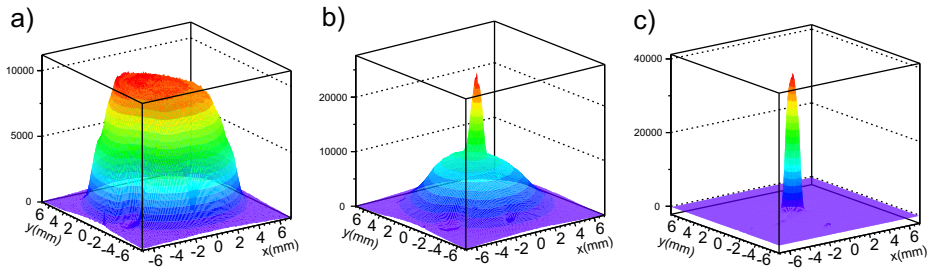

Fig. 3 Excitation of the diocotron mode of electrons. **a** no excitation; **b**, **c** displacement of the plasma with controlled phase. The amplitude D = 1.5 cm is consistent with that necessary to reach the nanoporous target. The radius of the big trap is 2.2 cm

Table 1 Summary of the energies obtained from the laser apparatus in the AEgIS working conditions

Transition	Wavelength	Saturation energy	Max. produced energy
$1 \rightarrow 3$	205 nm	32 μJ	106 μJ
$3 \rightarrow 26$	1664 nm	350 μJ	4000 μJ

The saturation energy was estimated with a 3mm-diameter beam. The produced energy was measured at the end of the fiber connecting the laser to the main cryostat

rest of antiprotons in silicon and in nuclear emulsions were detected and the results have been compared with nuclear fragmentation models [7, 14]. Particularly attractive is the use of nuclear emulsions offering a spatial resolution of 1–2 μm in the determination of the vertex of antihydrogen. An hybrid detector for the gravity measurement formed by the combination of silicon (having time resolution) and emulsion coupled to the grating is presently under design.

The successful coupling of a prototype of a moiré deflectometer to an emulsion based detector has been demonstrated during the 2012 antiproton run and it has been applied to a measurement of a small acceleration of slow antiprotons. Details of the system and the results are reported in [15]. The two gratings, mounted at the end of the 1 Tesla field, were 25 mm distant, 100 μm thick with a slit width of 12 μm and a periodicity of 40 μm. Antiprotons from AD reached the grating after traversing some foils used to decelerate them and to separate the vacuum chambers. The resulting antiproton mean energy, estimated with Geant4 based simulation, was about 100 KeV. The corresponding mean de Broglie wavelength is 8.8 10^{-14} m which implies that the concept of classical paths for the trajec-tories of the antiprotons is applicable. The emulsion detector was mounted at a distance of 25 mm from the second grating. The distribution of the annihilation points on the emul-sion is expected to show the same spatial periodicity of the grating. A force acting on the particles flying through the grating produces a shift of this periodical distribution. Abso-lute referencing of the observed antimatter pattern with a photon pattern (employing Talbot Lau interferometry) experiencing no deflection allowed the measurement of the force. The observed mean shift of 9.8 μm is consistent with a mean force of 530 aN due to residual magnetic fields acting on the antiprotons. The important point to be underlined is that the expected absolute shift of the antihydrogen pattern due to gravity in the final setup of AEgIS will be comparable to the one observed in the current experiment.

References

1. Wagner, T.A., et al.: Torsion-balance tests of the weak equivalence principle. Class. Quantum Grav. **29**, 184002 (2012)
2. Tasson, J.D.: Gravity effects on antimatter in the standard-model extension. Int. J. Mod. Phys. **30**, 1460273 (2014)
3. Drobychev, G., et al. (AEgIS Collaboration): Proposal for the AEGIS experiment at the CERN antiproton decelerator (Antimatter Experiment: Gravity, Interferometry, Spectroscopy). SPSC-P-334; CERN-SPSC-2007-017 (2007)
4. Mariazzi, S., et al.: Positronium cooling and emission in vacuum from nanochannels at cryogenic temperature. Phys. Rev. Lett. **104**, 243401 (2010)
5. Mariazzi, S., et al.: High positronium yield and emission into the vacuum from oxidized tunable nanochannels in silicon. Phys. Rev. B **81**, 235418 (2010)
6. Testera, G., et al. (AEgIS Collaboration): Formation of a cold antihydrogen beam in AEGIS for gravity measurements. AIP Conf. Proc. **1037**, 5 (2008)
7. Aghion, S., et al. (AEgIS Collaboration): Prospects for measuring the gravitational free-fall of antihydrogen with emulsion detectors. J. Instrum. **8**, P08013 (2013)
8. Di Domizio, S., et al.: Toward sub-Kelvin resistive cooling and non destructive detection of trapped non-neutral electron plasma, accepted by JINST
9. Kellerbauer, A., Walz, J.: A novel cooling scheme for antiprotons. New J. Phys. **8**, 45 (2006)
10. Surko, C.M., et al.: Positron plasma in the laboratory. Phys. Rev. Lett. **62**, 901 (1989)
11. Krasnický, D., et al. (AEgIS Collaboration): AEgIS experiment commissioning at CERN. AIP Conf. Proc. **1521**, 144 (2013)
12. Canali, C., et al.: Off-axial plasma displacement suitable for antihydrogen production in AEgIS experiment. EPJD **65**(3), 499 (2011)
13. Cialdi, S., et al.: Efficient two-step positronium laser excitation to Rydberg levels. NIM B **269**, 1527 (2011)
14. Aghion, S., et al. (AEgIS Collaboration): Detection of low energy antiproton annihilations in a segmented silicon detector. JINST **9**, P06020 (2014)
15. Aghion, S., et al. (AEgIS Collaboration): A moiré deflectometer for antimatter. Nat. Commun. **5**, 4538 (2014)